



**HAL**  
open science

## Parvalbumin interneuron-derived tissue-type plasminogen activator shapes perineuronal net structure

Matthieu Lépine, Sara Douceau, Gabrielle Devienne, Paul Prunotto, Sophie Lenoir, Caroline Regnauld, Elsa Pouette, Juliette Piquet, Laurent Lebouvier, Yannick Hommet, et al.

### ► To cite this version:

Matthieu Lépine, Sara Douceau, Gabrielle Devienne, Paul Prunotto, Sophie Lenoir, et al.. Parvalbumin interneuron-derived tissue-type plasminogen activator shapes perineuronal net structure. *BMC Biology*, 2022, 20, pp.218. 10.1186/s12915-022-01419-8 . hal-03807113

**HAL Id: hal-03807113**

**<https://hal.science/hal-03807113>**

Submitted on 9 Oct 2022

**HAL** is a multi-disciplinary open access archive for the deposit and dissemination of scientific research documents, whether they are published or not. The documents may come from teaching and research institutions in France or abroad, or from public or private research centers.

L'archive ouverte pluridisciplinaire **HAL**, est destinée au dépôt et à la diffusion de documents scientifiques de niveau recherche, publiés ou non, émanant des établissements d'enseignement et de recherche français ou étrangers, des laboratoires publics ou privés.




Distributed under a Creative Commons Attribution 4.0 International License

RESEARCH ARTICLE

Open Access



# Parvalbumin interneuron-derived tissue-type plasminogen activator shapes perineuronal net structure

Matthieu Lépine<sup>1†</sup>, Sara Douceau<sup>1†</sup>, Gabrielle Devienne<sup>2</sup>, Paul Prunotto<sup>1</sup>, Sophie Lenoir<sup>1</sup>, Caroline Regnaud<sup>1</sup>, Elsa Pouettré<sup>1</sup>, Juliette Piquet<sup>2</sup>, Laurent Lebouvier<sup>1</sup>, Yannick Hommet<sup>1</sup>, Eric Maubert<sup>1</sup>, Véronique Agin<sup>1</sup>, Bertrand Lambomez<sup>2</sup>, Bruno Cauli<sup>2</sup>, Carine Ali<sup>1\*†</sup>  and Denis Vivien<sup>3†</sup>

## Abstract

**Background:** Perineuronal nets (PNNs) are specialized extracellular matrix structures mainly found around fast-spiking parvalbumin (FS-PV) interneurons. In the adult, their degradation alters FS-PV-driven functions, such as brain plasticity and memory, and altered PNN structures have been found in neurodevelopmental and central nervous system disorders such as Alzheimer's disease, leading to interest in identifying targets able to modify or participate in PNN metabolism. The serine protease tissue-type plasminogen activator (tPA) plays multifaceted roles in brain pathophysiology. However, its cellular expression profile in the brain remains unclear and a possible role in matrix plasticity through PNN remodeling has never been investigated.

**Result:** By combining a GFP reporter approach, immunohistology, electrophysiology, and single-cell RT-PCR, we discovered that cortical FS-PV interneurons are a source of tPA *in vivo*. We found that mice specifically lacking tPA in FS-PV interneurons display denser PNNs in the somatosensory cortex, suggesting a role for tPA from FS-PV interneurons in PNN remodeling. *In vitro* analyses in primary cultures of mouse interneurons also showed that tPA converts plasminogen into active plasmin, which in turn, directly degrades aggrecan, a major structural chondroitin sulfate proteoglycan (CSPG) in PNNs.

**Conclusions:** We demonstrate that tPA released from FS-PV interneurons in the central nervous system reduces PNN density through CSPG degradation. The discovery of this tPA-dependent PNN remodeling opens interesting insights into the control of brain plasticity.

**Keywords:** Tissue-type plasminogen activator, Plasminogen, Parvalbumin interneurons, Perineuronal nets, Aggrecan

## Background

Perineuronal nets (PNNs) are a specific form of extracellular matrix (ECM), in which chondroitin sulfate proteoglycans (CSPGs), hyaluronan, link proteins, and tenascin-R are organized into dense lattice-like structures [26, 86]. In the cerebral cortex, PNNs mainly envelop fast-spiking parvalbumin (FS-PV) interneurons. They are formed during post-natal development and are thought to stabilize neuronal circuits at adult stages [12, 26, 89, 96]. Indeed, PNN digestion with the bacterial enzyme

<sup>†</sup>Matthieu Lépine, Sara Douceau, Carine Ali and Denis Vivien contributed equally to this work.

\*Correspondence: ali@cyceron.fr

<sup>1</sup> Normandie Univ, UNICAEN, INSERM, INSERM UMR-S U1237, Physiopathology and Imaging of Neurological Disorders, Institut Blood and Brain @ Caen Normandie, Cyceron, Bd Becquerel, BP 5229-14074, 14000 Caen, France  
Full list of author information is available at the end of the article



chondroitinase ABC (ChABC) strongly affects neuronal excitability and influences brain plasticity [2, 11, 30, 42, 62, 70, 76]. In the brain, endogenous proteases such as A Disintegrin And Metalloproteinase with Thrombospondin Motifs (ADAMTS) or matrix metalloproteinases (MMPs) may regulate PNN functions through the cleavage of their CSPGs, including aggrecan, neurocan, versican, and brevican [34, 86]. Paradigms of sensory deprivation have demonstrated the critical implication of PNN remodeling during periods of heightened plasticity, as well as the involvement of endogenous MMP9 in PNN plasticity [37, 59, 60, 66]. Interestingly, it has been shown that the expression and activity of the serine protease, tissue-type plasminogen activator (tPA) increase after sensory deprivation. Furthermore, tPA is thought to participate in plasticity-related mechanisms [16, 52, 53, 58]. However, a direct link between tPA-driven plasticity and PNNs remains unestablished.

In the (neuro-)vascular clinical community, tPA is well known as being the major enzymatic activator of plasminogen, thus promoting vascular fibrinolysis. Besides, tPA also has prominent effects in the central nervous system (CNS). As reviewed recently [87], many actions of tPA in the CNS rely on its proteolytic activity. Some functions occur independently of plasmin(ogen), via different receptors and binding partners which include laminin, low-density lipoprotein receptor-related proteins (LRPs), N-methyl-D-aspartate receptor (NMDAR), or some growth factor precursors. Via these multiple targets, tPA is a key player in CNS physiological and pathological processes (for recent reviews see [87, 98]). For instance, during development, tPA controls neuronal migration [64] and promotes axonal growth/synaptic plasticity [4, 67, 68, 82]. Later in life, tPA modulates learning and memory processes [5, 32, 48] and anxiety-related behaviors [54, 65]. Under pathological conditions, tPA controls neuronal death [44, 45, 61, 94], neuro-inflammation, and blood–brain barrier permeability [47, 55, 77, 81].

Consensual descriptions of the cellular distribution of tPA in the CNS are lacking. So far, most literature agrees that tPA can be released in the extracellular space by endothelial cells, oligodendrocytes, and hippocampal neurons [43, 46, 80]. Microglia and astrocytes are uncertain sources of tPA under physiological conditions but

might be under pathological conditions [1, 91]. In the CNS, tPA is easily detected (mRNA and protein) in hippocampal mossy fibers [46, 74, 85], but its immunohistological detection in cortical neurons is only available through its somatic accumulation after the blockade of axo-dendritic transport with colchicine. Interestingly, immunohistological (after colchicine injection), electrophysiological, and transcriptional analyses revealed the expression of tPA in a subset of excitatory neurons [46, 84]. tPA expression has also been suggested in some GABAergic interneurons in different brain areas [17, 28, 80].

In the present study, using a viral reporter construct, electrophysiology, and single-cell RT-PCR in mice, we found that cortical GABAergic neurons, mainly FS-PV interneurons, express tPA. Using conditional mice presenting a depletion of tPA restricted to PV cells, as well as primary culture of interneurons, we show that tPA originating from PV cells controls PNN turnover through plasmin. This regulation occurs through the cleavage of a component crucial for PNN structural integrity, the CSPG aggrecan.

## Results

### tPA is expressed by cortical fast-spiking parvalbumin interneurons in vivo

We sought to identify the cell subtypes expressing tPA in the somatosensory cortex of adult mice. We used a viral reporter construct encoding for green fluorescent protein (GFP) under the control of the human tPA (Plat) promoter (AAV-Plat-GFP, Fig. 1A). This construct was first validated in the dentate gyrus (DG; Additional file 1: Fig. S1A–B), a brain structure in which tPA expression is well described [46, 80]. After injection of the AAV-Plat-GFP in the somatosensory cortex, immunohistochemical analyses revealed that the GFP reporter was only detected in NeuN-positive neuronal cells but neither in GFAP-positive astrocytes nor in Iba-1-positive microglia (Fig. 1A; these three cell types are potential targets of AAV9-driven infection [50, 56]). Even under inflammatory conditions (lipopolysaccharide treatment), neither reactive astrocytes nor reactive microglia expressed GFP, excluding the expression of tPA in these cell types (Additional file 1: Fig. S2).

(See figure on next page.)

**Fig. 1** tPA is expressed by parvalbumin interneurons enwrapped with PNNs. **A** AAV-Plat-GFP was injected in the somatosensory cortex of adult wild-type mice. Co-immunohistochemistry of the GFP reporter (green) with the neuronal marker NeuN (magenta), the astrocyte marker GFAP (magenta), and the microglial marker Iba-1 (magenta) in the somatosensory cortex of adult WT mice 3 weeks after AAV injection. AAV-Plat-GFP induces expression of GFP in neurons but not in astrocytes or microglia (Scale bar: 100  $\mu$ m). **B,C** Co-localization of the Plat-GFP reporter (green) with GABA (cyan) and parvalbumin (magenta) markers following injection of AAV-Plat-GFP in the somatosensory cortex of WT mice (Scale bar: 100  $\mu$ m). Quantitative analysis of Plat-mediated expression of GFP in relation to GABAergic positive neurons and parvalbumin interneurons. **C** Around 37 % of Plat-GFP positive neurons are GABAergic interneurons and 73 % of them co-localized with PV marker ( $n=4$  coronal sections from  $N=3$  WT brains). **D** 3D reconstruction of a Plat-GFP positive neuron (green), co-labeled with PV (magenta) and the PNN marker Wisteria floribunda agglutinin (WFA, yellow) (Scale bar: 10  $\mu$ m). **E** Quantification of Plat-GFP neurons double stained with PV and WFA



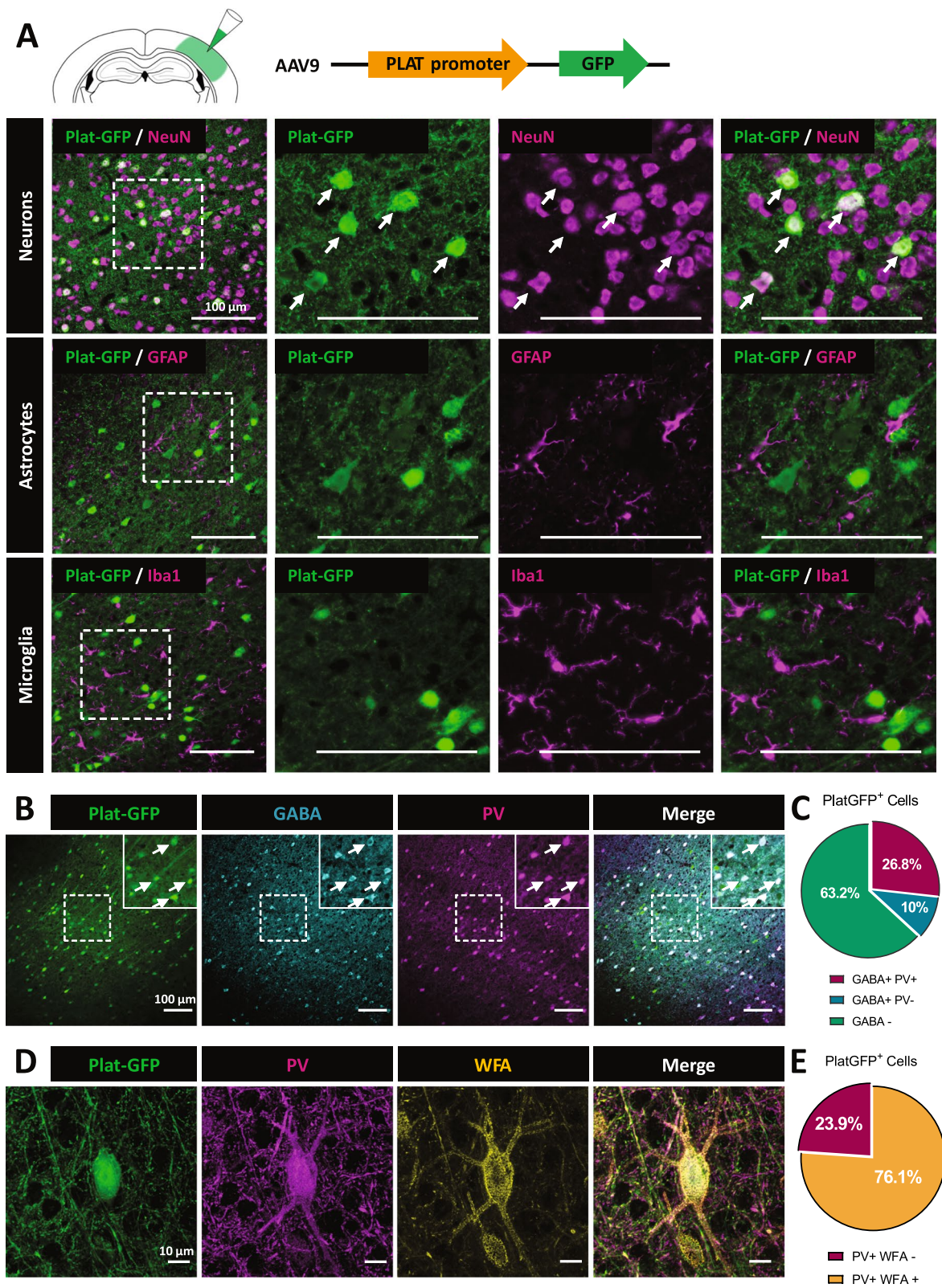


**Fig. 1** (See legend on previous page.)

Confirming our previous findings [46], a subset of tPA-GFP+ neurons were excitatory glutamatergic neurons, as they expressed *Tbr1* (Additional file 1: Fig. S3). In addition, we found that 36.9 % of Plat-GFP+ neurons were positive for GABA (Fig. 1B,C). Among these Plat-GFP GABAergic interneurons, the majority (72.7 %) were parvalbumin+ (Fig. 1B,C) and 76.1 % of these parvalbumin+ neurons were wrapped with PNNs (stained with WFA; Fig. 1D,E). In situ hybridization confirmed the presence of tPA mRNA in PV interneurons, and more precisely those wrapped by PNNs (Additional file 1: Fig. S4).

We also performed electrophysiological and molecular characterizations of 28 neurons from deeper layers (IV-V) of the mouse primary visual cortex by combining patch-clamp recordings and single-cell RT-PCR [13]. The PCR protocol was designed to probe the expression of different cell type-specific markers (*VGLUT1*, *GAD65* and *GAD67*, *PV*, *S100β*, *Sst*, *APC*, and *Akr1c18*), plasminogen activators (Plat: tPA gene and Plau: urokinase), and extracellular matrix-related genes (*Ncan*, *Ptprz1*, *Ptpr*, *Sema3a*, *Sdc4*, and *Mybpc1*; Additional file 1: Table S1). Pyramidal cells ( $n=14$ ) were identified by the triangular shape of their soma and their regular spiking firing pattern characterized by broad spikes and marked frequency adaptation. FS-PV interneurons of G42 mice (PV-expressing reporter mouse) [15] were characterized by low input resistance and high rheobase currents [36]. FS-PV interneurons fired short-duration action potentials with sharp post-hyperpolarizing potentials and were able to sustain a high firing rate with little or no spike frequency adaptation (Fig. 2A). The molecular analysis of the FS-PV interneuron shown in Fig. 2B confirmed the expression of *PV* and *GAD65/67*, as well as *SST*, *APC*, *Akr1c18*, *Plat*, *Ncan*, *Ptpr*, and *Sema3a*.

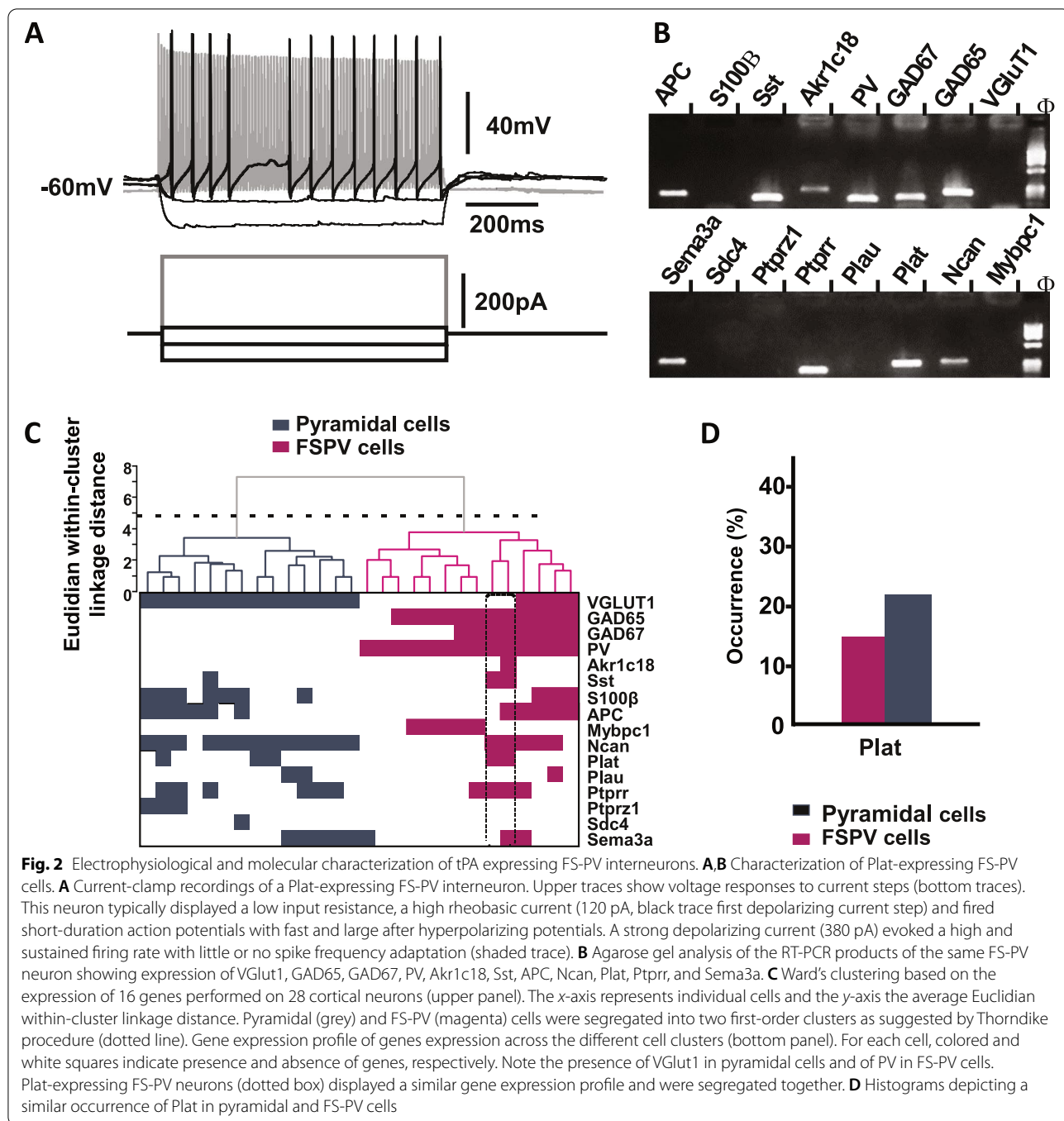
Analyzed neurons were grouped together according to their overall molecular similarity using Ward's clustering [14], yielding two main groups (Fig. 2C). All neurons in the left cluster were pyramidal cells expressing *VGLUT1* but none in either cluster expressed *GADs* or *PV*. By contrast, all neurons in the right cluster expressed *PV* and were identified as FS-PV interneurons. A sub-cluster of two FS-PV interneurons (dotted box, Fig. 2C) displayed a similar molecular profile with expression of *Sst*, *Plat*, *Ncan*, *Plat*, and *Ptpr*. *Plat* mRNA was detected in 14.3 % of FS-PV cells ( $n=2$  of 14 cells, Fig. 2D), a proportion similar to that observed in pyramidal cells (21.4 %,  $n=3$  of 14 cells,  $p=0.663$ ) and confirming our previous observations [46].

#### tPA produced by PV interneurons degrades surrounding PNNs in a plasmin-dependent manner (in vivo and in vitro investigations)

To assess the effect of tPA expressed by PV cells on the remodeling of PNNs, we generated a conditional knockout mouse strain lacking tPA in PV cells by crossing

tPA<sup>Flox<sup>+/+</sup></sup> mice with PV-Cre<sup>+/-</sup> mice (tPA<sup>Flox<sup>-/-</sup></sup>; PV-Cre<sup>+/-</sup> mice were used as controls, Additional file 1: Fig. S5). In both genotypes, the total number of PV interneurons, as well as the number of PV interneurons wrapped with PNNs, was similar (Fig. 3A–C). However, the overall intensity of WFA was higher in cKO mice than in WT mice (+14.4 %, Fig. 3D). A semi-quantitative analysis based on a qualitative grading PNN staining intensity around PV soma, from very low to very high WFA staining (Fig. 3E), revealed a slightly higher percentage of neurons wrapped with the highest degree of PNN coverage in cKO mice (Fig. 3F). Overall, these observations support the idea that tPA released from PV interneurons can contribute to PNN turnover in vivo.

To dissect the potential underlying mechanism of this effect, we used a model of primary murine interneuron cultures ([27]; Fig. 4). Immunocytochemistry confirmed the presence of PNN-like structures (displaying WFA labelling and expressing aggrecan and hyaluronic acid, two major components of PNN; Additional file 1: Fig. S6A) that were sensitive to ChABC (Additional file 1: Fig. S6B). We assessed PNN integrity in response to treatment with tPA alone or in combination with its conventional substrate plasminogen, plasminogen alone, or active plasmin (Fig. 4A,B). After 24h exposure, we observed a significant PNN degradation with plasmin treatment (−87.3%) or with the combination of plasminogen+tPA (−87.6%), while tPA alone did not alter PNN turnover (Fig. 4A,B). This suggests that tPA might not directly promote PNN degradation. Accordingly, aprotinin, a blocker of plasmin proteolytic activity, prevented plasminogen + tPA-induced PNN degradation (Additional file 1: Fig. S7A–B) demonstrating that tPA promotes PNN degradation via a plasmin-dependent mechanism. We found that plasminogen alone could also induce PNN degradation (−88.4 %; Fig. 4A,B), suggesting that endogenous tPA released by interneurons converts extracellular plasminogen into plasmin. To confirm this, a fluorescent assay of plasmin activity revealed the actual conversion of plasminogen in active plasmin in the absence of exogenous tPA treatment (Additional file 1: Fig. S7C–D). We also exposed cultured interneurons from tPA Null mice to plasminogen, plasmin, or plasminogen + tPA during 24 h (Fig. 4C,D). Although plasmin and plasminogen + tPA significantly reduced WFA staining (−88.2 % for plasmin; −91.5 % for plasminogen + tPA), plasminogen alone did not (Fig. 4C,D), confirming that PNN degradation depends on endogenous tPA produced by interneurons. We also found that plasmin-dependent degradation of PNNs in vitro was not sensitive to TIMP3 [90], suggesting that MMPs or ADAMTS are not downstream effectors in this pathway (Additional file 1: Fig. S8). To understand how plasmin promotes PNN



(See figure on next page.)

**Fig. 3** Specific deletion of tPA in PV interneurons affects PNNs morphology. **A** Representative images of PV cells (magenta) and PNNs (yellow) in the somatosensory cortex of adult tPAFllox<sup>+/+</sup>; PV-Cre<sup>+/-</sup> mice (cKO) and their control littermates (Ctrl), tPAFllox<sup>-/-</sup>; PV-Cre<sup>+/-</sup> mice (Scale bar: 100 μm). Quantitative analysis of the density of PV cells (**B**) and PNN-containing PV cells (**C**) in both genotypes. **D** Average WFA intensity was quantified in both groups. **E** PNNs were assigned to different categories based on the intensity of WFA staining (Scale bar: 10 μm). The percentage of each PNN subtype (**F**) and the graph show mean ± sem (N=5 animals; n=4 coronal sections per animal). Mann-Whitney test; \*: p<0.05



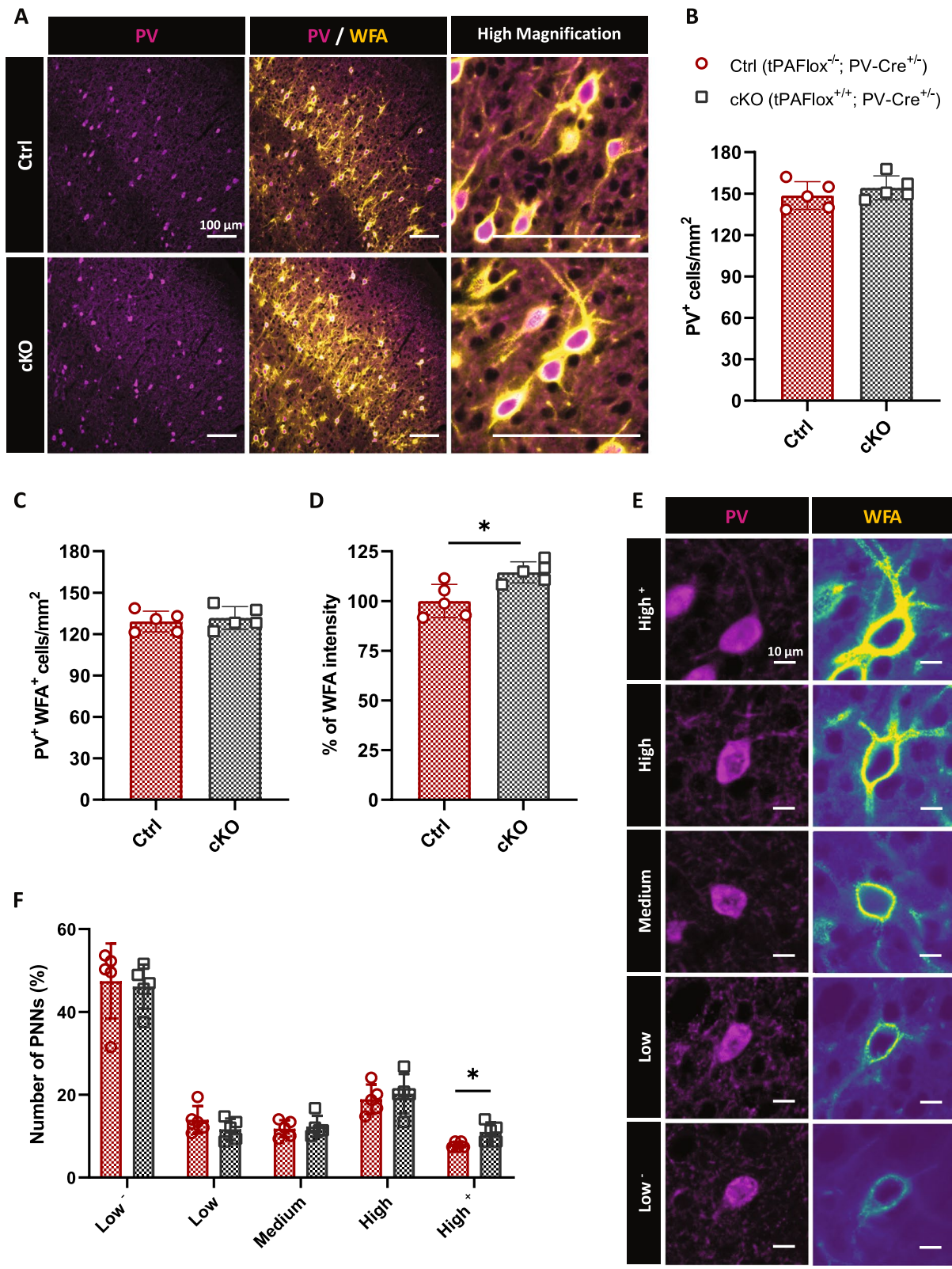


**Fig. 3** (See legend on previous page.)

degradation, we incubated a fragment of the aggrecan core protein (corresponding to G1-IGD-G2) with plasminogen, plasmin, tPA alone or in combination, and with or without aprotinin (Fig. 4E–G). ADAMTS-4 was used as a positive proteolytic control. Aggrecan core protein was efficiently cleaved by plasmin (51% loss in the signal of the core protein) and plasminogen + tPA (28.7 % loss in the signal of the core protein), leading to two fragments (55 and 65 kDa) which were similarly obtained with the control treatment with ADAMTS4 (–66%). Plasmin treatment also leads to two products of 90 and 30 kDa due to a second cleavage site. Moreover, as observed with WFA staining, a significant decrease of aggrecan staining around PV cells in vitro revealed that tPA-dependent activation of plasminogen degrades this perineuronal CSPG in situ (Fig. 4H,I).

## Discussion

The present study provides the first demonstration that tPA expressed by FS-PV interneurons regulates PNN remodeling, through the conversion of plasminogen into plasmin. This remodeling results from the cleavage of a major component of PNNs, the CSPG aggrecan.

tPA expression was previously reported in excitatory pyramidal neurons using in situ hybridization techniques, immunohistochemistry, and single-cell PCR coupled with patch-clamp recordings [46, 75]. Sparse and inconsistent studies have also reported tPA expression in some subtypes of GABAergic interneurons. Immunohistological studies [28] have reported tPA expression in VIP-positive, but not in SST-positive perivascular interneurons. Using a reporter mouse line, Stevenson and Lawrence discovered the specific expression of tPA in SST-positive oriens-lacunosum moleculare interneurons, a subpopulation of hippocampal interneurons responsible for synaptic plasticity in Shaffer collateral synapses [80]. Furthermore, the presence of tPA in PV-positive neurons but not in SST-positive neurons has been proposed

in the somatosensory cortex, although the specificity of the staining is not entirely clear [17]. One of our main findings is the demonstration by molecular, electrophysiological, and single-cell RT-PCR approaches that tPA is expressed by GABAergic interneurons, including FS-PV interneurons. These FS-PV interneurons are fundamental for several behavioral responses and their dysfunction participates in several diseases, including schizophrenia and autism [35, 73]. Interestingly, their activity is at least in part under the control of a specialized ECM that surrounds them, the PNNs. PNNs are dynamic structures, not only during experience-driven plastic developmental periods [51, 83, 96], but also in adults. For instance, modification of PNN density with the diurnal-nocturnal cycle, or their enzymatic degradation may have a potential impact on memory processing [30, 63, 78]. In line with this, memory-related diseases (Alzheimer's disease, drug addiction), but also many other pathological conditions (schizophrenia, epilepsy, depression, multiple sclerosis, stroke, Huntington's disease) may to some extent involve or impact PNN integrity and function [12, 23, 86, 93].

CSPGs, the major components of PNNs, are sensitive to endogenous processing by proteases of the MMP and ADAMTS families [34, 86]. FS-PV interneurons and pyramidal cells express an array of proteases that could thus process PNNs from both sides [21, 71]. Previous studies have shown that the tPA/plasmin system can degrade several CSPGs found in PNNs, such as neurocan, versican, and phosphacan [38, 95] and can activate pro-MMPs and pro-ADAMTS4 into their mature form [19, 41]. Interestingly, the tPA/plasmin system can also increase ChABC-mediated axonal regrowth after spinal cord injury through CSPG degradation [9]. However, the direct evidence of PNN degradation by the tPA/plasmin system has never been provided. Here, we show that the conditional deletion of tPA in FS-PV interneurons in vivo leads to a moderate increase in PNN density in the

(See figure on next page.)

**Fig. 4** Endogenous tPA controls the remodeling of PNNs through plasmin-dependent aggrecan cleavage. **A,B** MGE-derived WT interneuron cultures were treated at DIV14 with plasmin (200 nM), plasminogen (100 nM), tPA (10 and 200 nM), and processed 24h later for immunocytochemistry. **A** Representative images for PV (magenta) and WFA (yellow) stainings. **B** Quantification shows that plasmin, plasminogen, and plasminogen + tPA reduce WFA staining, whereas tPA has no effect. **C** Representative images of MGE-derived tPA Null interneuron cultures stained for PV (magenta) and WFA (yellow) 24h after treatment with plasmin (200 nM), plasminogen (100 nM), and tPA (10 nM). **D** WFA-positive area quantification reveals that plasmin induces the degradation of PNN in PV cells from tPA Null cultures whereas plasminogen fails to (mean  $\pm$  sem;  $n=40$  cells from 4 independent experiments). Kruskal-Wallis test followed by Dunn's post hoc test for multiple comparisons; ###:  $p<0.001$  (compared to control), \*\*\*:  $p<0.001$  (compared to plasminogen + tPA). Scale bar: 10  $\mu$ m. **E–G** Human aggrecan G1-G2 (156 nM) was incubated with ADAMTS4 (positive control), plasmin, plasminogen, tPA (7.8 nM for each protease), and aprotinin (78 nM) overnight. **F,G** Degradation products were visualized by Imperial blue staining. Like ADAMTS4, plasmin, and plasminogen + tPA can cleave aggrecan G1-G2 in vitro. Aprotinin reverses plasmin-dependent aggrecan degradation.  $N=4$  independent experiments. One-way ANOVA, Fisher's LSD post hoc test; #:  $p<0.05$ ; ##:  $p<0.01$ ; ###:  $p<0.001$  (compared to Agg G1-G2). **H** Representative images of MGE-derived WT interneuron cultures treated with plasmin (100 nM), plasminogen (100 nM), and tPA (10 and 200 nM) and co-stained with aggrecan (cyan) and PV (magenta). **I** Quantitative analysis of aggrecan positive area shows that plasmin, plasminogen, and plasminogen + tPA reduce aggrecan staining whereas tPA treatment has no effect in WT interneurons (mean  $\pm$  sem;  $n=40$  cells from 4 independent experiments). Kruskal-Wallis test followed by Dunn's post hoc test for multiple comparisons; ###:  $p<0.001$  (compared to Control). Scale bar: 10  $\mu$ m



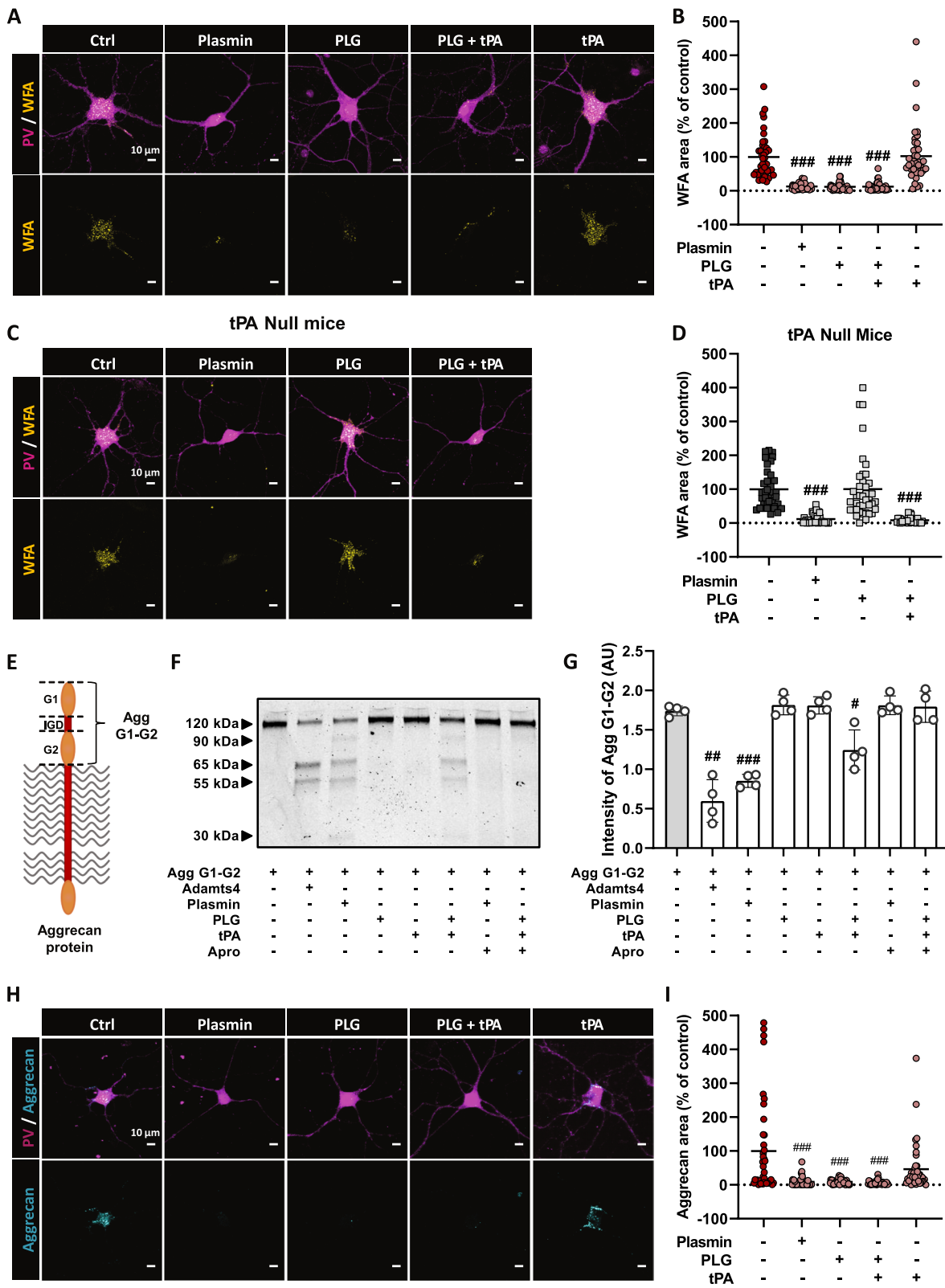


**Fig. 4** (See legend on previous page.)

somatosensory cortex, which is indicative of a cell-autonomous regulation of PNN plasticity under physiological conditions. Thus, the histological modifications observed *in vivo* under basal conditions could reflect modifications of the dynamic balance between CSPG synthesis and their degradation. However, using *in vitro* experiments, by combining cell imaging and pharmacology, we demonstrate that tPA indeed promotes PNN degradation around PV interneurons through plasminogen conversion into plasmin. The latter can be blocked by aprotinin and is independent of MMP or ADAMTS activation, since a broad-range inhibitor (TIMP3) did not reverse the effects of plasmin. Overall, our study shows that tPA/plasmin can exert a cell-autonomous effect on PNN degradation when expressed by PV interneurons. Moreover, since tPA was described to be induced as an immediate early gene following seizure or long-term potentiation [68], we can hypothesize that its expression may be also triggered in PV cells under certain conditions to promote PNN remodeling. In addition, considering that tPA is also expressed in the brain by various cell types including pyramidal cells [46] or oligodendrocytes [43], it could also probably drive PNN degradation through a non-cell autonomous manner when released in the extracellular space.

The consequence of PNN degradation on FS-PV cell function has been the subject of several studies, sometimes with contradictory results [2, 22, 24, 25, 31]. For instance, PNN digestion induced by chondroitinase ABC was shown to reduce [2] or increase the excitability of interneurons [22]. However, these discrepancies could be explained by the experimental approaches used. Indeed, genetic removal of specific PNN components might affect the development of neuronal networks, which is not the case when PNN are acutely digested in the adult brain. Additionally, *in vitro* models cannot reflect the complexity of neuronal networks. It would be relevant to perform fine electrophysiological studies to determine the impact of tPA-driven degradation of PNN on PV cell functions. Furthermore, it has been described that the activity of PV cells and the density of PNNs influence fear memory and social behaviors [3, 6, 8, 18, 69, 79]. Therefore, it would also be interesting to investigate the consequence of PNN degradation by the tPA/plasmin, using PV-Cre x tPA flox mice, on these behavioral responses.

Finally, we also demonstrate that tPA-mediated PNN degradation can occur through the cleavage of the core protein of aggrecan. However, we cannot exclude that the plasminogen activator system may also promote PNN degradation through the cumulative cleavage of different CSPG as previously mentioned [38, 95]. Nevertheless, given that aggrecan is one of the main component of PNNs, we can hypothesize that plasmin is more likely

to influence PNN remodeling by acting on this particular CSPG. Indeed, aggrecan was shown to play a crucial role in PNN structure since its conditional knockout in the brain results in complete PNN loss in the cortex and the reactivation of juvenile plasticity [72]. Interestingly, both tPA and plasmin are also involved in plasticity-related mechanisms such as ocular dominance shift and dendritic spine remodeling during the critical period [52, 53]. In view of these results, we hypothesize that PNN degradation by the tPA/plasmin system could promote the restoration of juvenile plasticity under pathological conditions.

## Conclusions

In summary, our findings show that in the presence of plasminogen, tPA released from FS-PV cells reduces PNN density through CSPG degradation. This could affect several PNN properties, including balancing GABAergic and glutamatergic neurotransmissions [2, 22, 42, 70, 76, 78], being a physical protective barrier [10, 29, 57], a contributor to pathogenic pathways [40, 49, 62, 97], and a driver of synaptic plasticity and behavioral outcome [11, 29, 70, 76]. Overall, we provide unanticipated mechanistic insights in the regulation of PNNs with relevance to neuronal function, which could translate into new targets to promote plasticity/recovery under pathological conditions.

## Methods

### Animals

All experiments were conducted in accordance with the French ethical law (Decree 2013-118) and the European Communities Council guidelines (2010/63/EU). Protocols were approved by our local ethics committee dependent on the French Ministry of Research and Higher Education (agreement numbers Cenomexa #25267 and Ce5/2012/062). All applicable international, national, and/or institutional guidelines for the care and use of animals were followed. Electrophysiological experiments were performed on G42 transgenic mice (Jackson laboratories #007677, GAD67-GFP, 50). Histological analyses were performed on 8-week-old male Swiss mice, tPAFlox<sup>+/+</sup> mice, tPAFlox<sup>+/+</sup>; PV-Cre<sup>+/-</sup> mice and their control (tPAFlox<sup>-/-</sup>; PV-Cre<sup>+/-</sup>) littermates (20-25g). Pregnant tPA Null mice and their WT littermates at gestational day 14 were used for *in vitro* neuronal cultures.

Animals were housed with a 12-h light/12-h dark cycle with free access to water and food.

tPA Null mice were generated by the Mouse Clinical Institute (ICS, Illkirch, France). Briefly tPAFlox<sup>+/+</sup> mice (on a C57BL6NTac genetic background) in which exon 3 is flanked by loxP sites (see 3) were crossed with Rosa<sup>26</sup>-Cre mice [7] to induce Cre-mediated excision

of the third exon in germline. Mice were genotyped by PCR analysis and southern blots, using tail genomic DNA samples, to detect the presence/absence of loxP sequences. PV-Cre<sup>+/-</sup> female mice (Jackson laboratory # 008069, Pvalb<sup>tm1(cre)</sup>Arbr, [33]) were crossed with tPAFlox<sup>+/+</sup> male mice or tPAFlox<sup>-/-</sup> male mice to generate tPAFlox<sup>+/+</sup>; PV-Cre<sup>+/-</sup> (cKO) and their control littermates tPAFlox<sup>-/-</sup>; PV-Cre<sup>+/-</sup>. Mice were genotyped by PCR for the presence of loxP sites and Cre transgene.

#### Whole-cell recordings in acute slices

G42 mice were deeply anesthetized with isoflurane. After decapitation, brains were quickly removed and placed into ice-cold oxygenated artificial cerebrospinal fluid (aCSF) containing (in mM): 126 NaCl, 2.5 KCl, 1.25 NaH<sub>2</sub>PO<sub>4</sub>, 2 CaCl<sub>2</sub>, 1 MgCl<sub>2</sub>, 26 NaHCO<sub>3</sub>, 10 glucose, 15 sucrose, and 1 kynurenic acid (Sigma). Coronal slices (300 μm thick) containing the primary visual cortex were cut with a vibratome (VT1000S; Leica) and allowed to recover at room temperature for at least 30 min in aCSF saturated with O<sub>2</sub>/CO<sub>2</sub> (95 %/5 %). Patch pipettes (4–6 MΩ) pulled from borosilicate glass were filled with 8 μl of RNase-free internal solution containing in mM: 144 K-gluconate, 3 MgCl<sub>2</sub>, 0.5 EGTA, 10 HEPES, pH 7.2 (285/295 mOsm). Whole-cell recordings were performed at room temperature using a patch-clamp amplifier (MultiClamp 700B, MDS). Membrane potentials were not corrected for liquid junction potential. Data were filtered at 10 kHz and digitized at 20 kHz using an acquisition board (Digidata 1440, MDS). Cells were set at -60 mV by continuous current injection and submitted to current pulses (800 ms, from -100 to 280 pA with 20 pA increments).

#### Cytoplasm harvesting and scRT-PCR

At the end of the whole-cell recording, lasting <15 min, the cytoplasmic content was harvested in the recording pipette. The content of the pipette was expelled into a test tube and RT was performed in a final volume of 10 μL, as described previously [39]. The scRT-PCR protocol was designed to probe simultaneously the expression of neuronal markers and key molecular elements including tissue-type plasminogen activator gene, Plat. Two-step amplification was performed essentially as described [13, 20]. Briefly, cDNAs present in the 10 μL reverse transcription reaction were first amplified simultaneously using all external primer pairs (Additional file 1: Table S1). Taq polymerase (2.5 U; Qiagen) and 20 pmol of each primer were added to the buffer supplied by the manufacturer (final volume, 100 μl), and 20 cycles (94°C, 30 s; 60°C, 30 s; and 72°C, 35 s) of PCR were run. Second rounds of PCR were performed using 1 μl of the first PCR product as a template. In this second round, each

amplicon was individually re-amplified using its specific nested primer pair (Additional file 1: Table S1) by performing 35 PCR cycles as described above. Ten microliters of each individual PCR product was run on a 2 % agarose gel stained with ethidium bromide using ΦX174 digested by *Hae*III as a molecular weight marker.

#### Unsupervised clustering

To classify cells, unsupervised clustering was performed using 16 molecular parameters (VGlut1, Gad65, Gad67, PV, Akr1c18, Sst, S100β, APC, Mybpc1, Ncan, Plat, Plau, Ptpr, Ptprz1, Sdc4, Sema3a). The presence of a given gene was digitized by 1 and its absence was digitized by 0. Ward-linkage hierarchical clustering [92] was performed and plotted as a dendrogram using “scipy.cluster.hierarchy” functions on Python 3.7. The final number of clusters was suggested by the Thorndike procedure [88] as described previously [14].

#### Viral production

Viral particles were provided by Gilles Bonvento and Alexis Bemelmans (INSERM U1169/MIRCen CEA, Fontenay aux Roses 92265, France).

The clone encoding for a GFP under the control of a 1.2-kb sequence of the Human Plat promoter (spanning from -1035 to +207 bp from the transcription start codon) was purchased from GeneCopoeia (pPlat-GFP; Catalog No.: HPRM12655-PF02). The pPlat-GFP was then subcloned in the pDONR221 for AAV production. All the constructs were amplified in *Escherichia coli* JM109 cells and purified by a Nucleobond endotoxin-free plasmid DNA PC 2000 kit (Macherey-Nagel) according to the manufacturer's instructions. The vector used for this study was an AAV9 serotype. Self-complementary AAV vectors expressing the Plat-GFP construct were produced by transfecting HEK293 cells with the adenovirus helper plasmid (pXX6-80), the AAV packaging plasmid carrying the rep2 and the cap8 genes, and the AAV2 shuttle plasmid containing the Plat-GFP transgene in a sc genome. Recombinant vectors (rAAV) were purified by ultracentrifugation on a discontinuous iodixanol density gradient followed by dialysis against the formulation buffer of the vector stocks, 0.5 mmol/l MgCl<sub>2</sub> and 1.25 mmol/l KCl in phosphate-buffered saline (PBSMK; five buffer changes, 3 h per round of dialysis). Physical particles were quantified by real-time PCR. Vector titers are expressed as viral genomes per milliliter (vg/mL).

#### Stereotaxic injection of AAV virus

Animals were deeply anesthetized with isoflurane 5 % and maintained with 2 % isoflurane in a 70 %/30 % mixture of NO<sub>2</sub>/O<sub>2</sub> in a stereotaxic frame (Harvard Apparatus). AAV9-Plat-GFP (1.25.10<sup>13</sup> vp/mL) were injected



through a glass micropipette in the right hemisphere in a volume of 0.5  $\mu$ L at a rate of 0.2  $\mu$ L/min. Coordinates (relative to bregma) according to the Paxinos Mouse Brain Atlas were as follows: AP:  $-0.25$  mm; ML:  $-3.4$  mm; DV:  $-0.4$  mm and  $-0.8$  mm for the somatosensory cortex. The needle was left in position for a further 5 min and then removed slowly from the brain. After recovery from surgery, mice were left undisturbed for 3 weeks for effective and stable transgene expression.

### Antibodies

The following antibodies, lectins, and biotinylated protein were used: mouse anti-NeuN (1:800, MAB377, Merck); anti-GFP (rabbit, 1:1000, ab6556, abcam or chicken, 1:1000, ab13970, abcam); chicken anti-Glial Fibrillary Acidic Protein (GFAP) (1:2000, ab4674, abcam); rabbit anti-ionized calcium-binding adapter molecule-1 (Iba-1) (1:1000, 019-19741, Fujifilm); rabbit anti-GABA (1:500, A2052, Sigma Aldrich); anti-parvalbumin (rabbit, 1:3000, ab 11427, abcam or guinea pig, 1:500, GP72, Swant); rabbit anti-aggregran (1:1000, AB1031, Merck); or Biotinylated Wisteria floribunda Agglutinin (WFA) (1:1000, L1516, Sigma Aldrich).

### Immunohistochemistry

Mice were deeply anesthetized with isoflurane 5 % in 70 %/30 % mixture of  $\text{NO}_2/\text{O}_2$ . A transcardial perfusion was performed with ice-cold 0.9 % NaCl with 3 % heparin followed by 150 ml of fixative solution containing 4 % paraformaldehyde (in PBS 0.1M, pH 7.4). Brains were removed and cryoprotected in 20 % sucrose solution (in PBS 0.1M, pH 7.4) for 24h and frozen in Tissue-Tek (Miles Scientific). Cryostat sections of 10  $\mu$ m were collected on Poly-Lysine slides and stored at  $-80^\circ\text{C}$ . Sections were incubated overnight at room temperature with primary antibodies. Corresponding Fab'2-conjugated secondary antibodies were diluted at 1:800 (Jackson ImmunoResearch). Images were acquired using Leica DM6000 microscope-coupled CoolSnap camera, visualized with Metamorph 7.0 software (Molecular Devices), and further processed were realized using ImageJ software.

For 3D reconstruction, images were acquired using Leica TCS SP8 Confocal/STED 3  $\times$  microscope with an oil-immersion  $\times 40$ , 1.44-N.A. objective at a resolution of  $512 \times 512$  pixels with 572 Hz speed and a step size of 0.22  $\mu$ m.

### Histological analysis

To estimate the percentage of each Plat-GFP cell, all transfected cells were quantified ( $1090.3 \pm 58.9$  Plat-GFP cells/brain, from four sections per brain, 3 WT mice). For PNN/PV cells quantification, 2 images per section

were acquired to cover all layers of the somatosensory cortex with a good resolution (four sections per brain, five mice per condition). PNN intensity was calculated as the intensity of WFA staining through the entire section of the somatosensory cortex. The overall intensity of WFA staining considers the high WFA staining around the soma and proximal dendrites and low WFA staining found around dendrites. PNN morphology was evaluated using a qualitative classification, ranging from High+ (strong WFA staining) to Low- (faint WFA staining). Only cells of which the soma was in the focal plane were classified. Analyses were performed blind to genotype.

### Primary cultures of interneurons

GABAergic interneurons derived from the medial ganglionic eminence (MGE) were prepared from fetal mice (embryonic day 14) as previously described [27]. Medial ganglionic eminences were dissected in HBSS (Hanks' Balanced Salt Solution, Gibco) /HEPES 10mM, incubated 15 min at  $37^\circ\text{C}$  in HBSS/HEPES with trypsin (0.05 %, Gibco) and DNase I (100  $\mu\text{g}/\text{mL}$ , Worthington) and mechanically dissociated through a glass pipette. Then, cells were plated (425,000 cells/mL) on glass bottom microwell dishes (MatTek Corporation) or on 24-well plates (500,000 cells/mL) previously coated with poly-D-lysine (0.1 mg/mL, Sigma Aldrich, P6407-5MG) and laminin (0.02 mg/mL, Gibco) in Neurobasal medium (Life Technologies) containing 2 % B27 supplement (Life Technologies) and 1 % Glutamax (Life Technology). Cytosine  $\beta$ -D-arabinofuranoside hydrochloride (5  $\mu\text{M}$ , Sigma Aldrich) was added at DIV3, and fresh medium was added at DIV7.

### In vitro treatments

Cells were treated at DIV14 with either 100 nM Human Glu-plasminogen (Enzyme Research Laboratories, HPg 2001), 200 nM Human Plasmin (Enzyme Research Laboratories, HPlasmin), or 10 nM or 200 nM Human tPA (Actilyse<sup>®</sup>, Boehringer Ingelheim) for 24 h.

### Immunocytochemistry

Cells were fixed during 10 min in 0.1 M PBS containing 4 % paraformaldehyde. After PBS washes, cells incubated for 1 h in PBS-Triton 0.25 % containing 1 % BSA and then incubated overnight at  $4^\circ\text{C}$  in blocking buffer containing primary antibodies. Confocal images were acquired with a Leica TCS SP8 Confocal/STED 3  $\times$  microscope with an oil-immersion  $\times 40$ , 1.44-N.A. objective. Confocal images were taken at a resolution of  $1024 \times 1024$  pixels with 400 Hz speed and a step size of 0.45  $\mu$ m. Laser intensity, gain, and offset were maintained constant in each analysis.

### PNN quantification in vitro

Confocal images were analyzed with the ImageJ software. Random PV-positive cells were imaged with  $160 \times 160 \times 15 \mu\text{m}$  z-stack with  $0.45 \mu\text{m}$  step size. A threshold was applied to the WFA channel or aggrecan channel (range 0–255), and the area was quantified in 40 neurons from 4 independent experiments.

### Enzymatic degradation assays

Recombinant human aggrecan core protein G1-IGD-G2 (156 nM) (Biotechne) was incubated at  $37^\circ\text{C}$  overnight with either 7.8 nM recombinant human ADAMTS4 protein (Biotechne), purified human plasmin (Enzyme Research Laboratories), Human Glu-plasminogen (Enzyme Research Laboratories), and/or tPA (Actilyse) in a buffer containing 50 mM Tris, 10mM  $\text{CaCl}_2$ , 150 mM NaCl, and 0.05 % Brij35. Then, 78 nM Aprotinin treatment was applied with either Glu-plasminogen + tPA treatment or plasmin treatment. Digestion products were analyzed by SDS-PAGE on 10 % Tris-Glycine gel and stained with GelCode Imperial Blue Stain Reagent (Pierce).

### Statistics

For sc-PCR analyses, between-group comparisons were performed using Mann–Whitney nonparametric test. Comparison of the occurrence of expressed genes between cell types was determined using Fisher's exact test. A *p*-value below 0.05 was considered statistically significant.

Otherwise, experiments were analyzed by investigators blinded to group allocation. Unblinding was made after completion of statistical analysis. All statistical analyses were performed using the GraphPad Prism 8 software. Comparisons between more than two independent samples were performed using two-tailed Kruskal–Wallis test and appropriate post hoc test (Dunn's test). Mann–Whitney *U* test was used for the comparisons of two independent samples. Plasmin activity was analyzed using 2-way Anova (two-stage linear step-up procedure of Benjamini, Krieger and Yekutieli). Recombinant aggrecan degradation was analyzed using one-way ANOVA followed by Fisher's LSD test. The intensity of the 120-kDa band was compared between Agg G1-G2 and protease-treated conditions. A threshold of  $P < 0.05$  was defined as statistically significant. All graph data are presented as the mean standard error mean (SEM). Sample sizes are indicated in each corresponding legend.

### Abbreviations

AAV: Adeno-associated viruses; ADAMTS: A Disintegrin And Metalloproteinase with Thrombospondin Motifs; CSPGs: Chondroitin sulfate proteoglycans; ECM: Extracellular matrix; FS-PV: Fast-spiking parvalbumin; GABA: Gamma-aminobutyric acid; LRP: Low-density lipoprotein receptor-related proteins; MMPs: Matrix metalloproteinases; NMDAR: N-methyl-D-aspartate receptor; PNN: Perineuronal nets; PV: Parvalbumin; TIMP3: Tissue inhibitor of metalloproteinases-3; tPA: Tissue-type plasminogen activator; VIP: Vasointestinal peptide; WFA: Wisteria floribunda agglutinin.

### Supplementary Information

The online version contains supplementary material available at <https://doi.org/10.1186/s12915-022-01419-8>.

**Additional file 1: Figure S1.** Characterization of a tPA-reporter viral construct in the dentate gyrus. **Figure S2.** Plat-GFP reporter expression in the cortex after LPS treatment. **Figure S3.** Plat-GFP reporter expression in excitatory neurons in the cortex. **Figure S4.** tPA mRNA is expressed in PV interneurons enwrapped with PNNs. **Figure S5.** Conditional depletion of tPA in PV interneurons. **Figure S6.** PNN-like structures *in vitro*. **Figure S7.** Interneuron-derived tPA promotes PNN degradation through plasmin. **Figure S8.** tPA/plasmin mediated PNNs degradation is MMP-independent. **Table S1.** Sequences of PCR primers. **Supplementary materials and methods.**

### Acknowledgements

We are grateful to Dr Mario Merlini for his helpful comments and corrections. We are grateful to Pr Gilles Bonvento and Dr Alexis-Pierre Bemelmans for viral particle production.

### Authors' contributions

DV and CA designed and supervised the study. ML, SD, GD, and PP performed the data analysis. ML, SD, GD, PP, SL, CR, EP, JP, YH, LL, and EM performed the experiments. ML, SD, GD, PP, CA, BL, BC, VA, and DV wrote the manuscript. All authors have read and approved the final manuscript.

### Funding

This work was funded by the Agence Nationale de la Recherche (Projet-ANR-15-CE16-0010), the Institut National de la Santé Et de la Recherche Médicale, Caen Normandy University and the Regional Council of Normandy.

### Availability of data and materials

All data generated or analyzed during this study are included in this published article and its supplementary information files. All data supporting our results are available from the corresponding author upon reasonable request.

### Declarations

#### Ethics approval and consent to participate

All experiments were conducted in accordance with the French ethical law (Decree 2013-118) and the European Communities Council guidelines (2010/63/EU).

#### Consent for publication

Not applicable.

#### Competing interests

The authors declare that they have no competing interests.

#### Author details

<sup>1</sup>Normandie Univ, UNICAEN, INSERM, INSERM UMR-S U1237, Physiopathology and Imaging of Neurological Disorders, Institut Blood and Brain @ Caen Normandie, Cycleron, Bd Becquerel, BP 5229-14074, 14000 Caen, France.

<sup>2</sup>Neuroscience Paris Seine - Institut de Biologie Paris Seine (NPS - IBPS), Sorbonne Université UM119, CNRS UMR8246, INSERM U1130, 75005 Paris, France.

<sup>3</sup>Department of clinical research, CHU de Caen Normandie, Caen, France.

Received: 2 November 2021 Accepted: 27 September 2022  
Published online: 05 October 2022

## References

- Adhami F, Yu D, Yin W, Schloemer A, Burns KA, Liao G, et al. Deleterious effects of plasminogen activators in neonatal cerebral hypoxia-ischemia. *Am J Pathol.* 2008;172:1704–16. <https://doi.org/10.2353/ajpath.2008.070979>.
- Balmer TS. Perineuronal nets enhance the excitability of fast-spiking neurons. *eNeuro.* 2016;3:1–13. <https://doi.org/10.1523/ENEURO.0112-16.2016>.
- Banerjee SB, Gutzeit VA, Baman J, Aoued HS, Doshi NK, Liu RC, et al. Perineuronal nets in the adult sensory cortex are necessary for fear learning. *Neuron.* 2017;95:169–179.e3. <https://doi.org/10.1016/j.neuron.2017.06.007>.
- Baranes D, Lederfein D, Huang VY, Chen M, Bailey CH, Kandel ER. Tissue plasminogen activator contributes to the late phase of LTP and to synaptic growth in the hippocampal mossy fiber pathway. *Neuron.* 1998;21:813–25. [https://doi.org/10.1016/S0896-6273\(00\)80597-8](https://doi.org/10.1016/S0896-6273(00)80597-8).
- Benchenane K, Castel H, Boulouard M, Bluthé R, Fernandez-Monreal M, Roussel BD, et al. Anti-NR1 N-terminal-domain vaccination unmasks the crucial action of tPA on NMDA-receptor-mediated toxicity and spatial memory. *J Cell Sci.* 2007;120:578–85. <https://doi.org/10.1242/jcs.03354>.
- Bicks LK, Yamamuro K, Flanigan ME, Kim JM, Kato D, Lucas EK, et al. Prefrontal parvalbumin interneurons require juvenile social experience to establish adult social behavior. *Nat Commun.* 2020;11. <https://doi.org/10.1038/s41467-020-14740-z>.
- Birling MC, Dierich A, Jacquot S, Hérault Y, Pavlovic G. Highly-efficient, fluorescent, locus directed cre and FlpO deleter mice on a pure C57BL/6N genetic background. *Genesis.* 2012;50:482–9. <https://doi.org/10.1002/dvg.20826>.
- Brown JA, Ramikie TS, Schmidt MJ, Báldi R, Garbett K, Everheart MG, et al. Inhibition of parvalbumin-expressing interneurons results in complex behavioral changes. *Mol Psychiatry.* 2015;20:1499–507. <https://doi.org/10.1038/mp.2014.192>.
- Bukhari N, Torres L, Robinson JK, Tsirka SE. Axonal regrowth after spinal cord injury via chondroitinase and the tissue plasminogen activator (tPA)/ plasmin system. *J Neurosci.* 2011;31:14931–43. <https://doi.org/10.1523/JNEUROSCI.3339-11.2011>.
- Cabungcal JH, Steullet P, Morishita H, Kraftsik R, Cuenod M, Hensch TK, et al. Perineuronal nets protect fast-spiking interneurons against oxidative stress. *Proc Natl Acad Sci U S A.* 2013;110:9130–5. <https://doi.org/10.1073/pnas.1300454110>.
- Carstens KE, Phillips ML, Pozzo-Miller L, Weinberg RJ, Dudek SM. Perineuronal nets suppress plasticity of excitatory synapses on CA2 pyramidal neurons. *J Neurosci.* 2016;36:6312–20. <https://doi.org/10.1523/JNEUROSCI.0245-16.2016>.
- Carulli D, Verhaagen J. An extracellular perspective on CNS maturation: Perineuronal nets and the control of plasticity. *Int J Mol Sci.* 2021;22:1–26. <https://doi.org/10.3390/ijms22052434>.
- Cauli B, Audinat E, Lambolez B, Angulo MC, Ropert N, Tsuzuki K, et al. Molecular and physiological diversity of cortical nonpyramidal cells. *J Neurosci.* 1997;17:3894–906. <https://doi.org/10.1523/jneurosci.17-10-03894.1997>.
- Cauli B, Porter JT, Tsuzuki K, Lambolez B, Rossier J, Quenet B, et al. Classification of fusiform neocortical interneurons based on unsupervised clustering. *Proc Natl Acad Sci U S A.* 2000;97:6144–9. <https://doi.org/10.1073/pnas.97.11.6144>.
- Chattopadhyaya B, Di Cristo G, Higashiyama H, Knott GW, Kuhlman SJ, Welker E, et al. Experience and activity-dependent maturation of perisomatic GABAergic innervation in primary visual cortex during a postnatal critical period. *J Neurosci.* 2004;24:9598–611. <https://doi.org/10.1523/JNEUROSCI.1851-04.2004>.
- Chen CC, Chu P, Brumberg JC. Experience-dependent regulation of tissue-type plasminogen activator in the mouse barrel cortex. *Neurosci Lett.* 2015;599:152–7. <https://doi.org/10.1016/j.neulet.2015.05.050>.
- Chu P, Chen E, Bajnath A, Brumberg JC. Cell type specificity of tissue plasminogen activator in the mouse barrel cortex. *Data Br.* 2015;4:332–5. <https://doi.org/10.1016/j.dib.2015.06.008>.
- Cope EC, Zych AD, Katchur NJ, Waters RC, Laham BJ, Diethorn EJ, et al. Atypical perineuronal nets in the CA2 region interfere with social memory in a mouse model of social dysfunction. *Mol Psychiatry.* 2021. <https://doi.org/10.1038/s41380-021-01174-2>.
- Davis GE, Pintar Allen KA, Salazar R, Maxwell SA. Matrix metalloproteinase-1 and -9 activation by plasmin regulates a novel endothelial cell-mediated mechanism of collagen gel contraction and capillary tube regression in three-dimensional collagen matrices. *J Cell Sci.* 2001;114:917–30.
- Devienne G, Le Gac B, Piquet J, Cauli B. Single cell multiplex reverse transcription polymerase chain reaction after patch-clamp. *J Vis Exp.* 2018;1–12. <https://doi.org/10.3791/57627>.
- Devienne G, Picaud S, Cohen I, Piquet J, Tricoire L, Testa D, et al. Regulation of perineuronal nets in the adult cortex by the electrical activity of parvalbumin interneurons: Cold Spring Harbor Laboratory; 2019.
- Dityatev A, Brückner G, Dityateva G, Grosche J, Kleene R, Schachner M. Activity-dependent formation and functions of chondroitin sulfate-rich extracellular matrix of perineuronal nets. *Dev Neurobiol.* 2007;67:570–88. <https://doi.org/10.1002/dneu.20361>.
- Dzyubenko E, Manrique-Castano D, Kleinschnitz C, Faissner A, Hermann DM. Topological remodeling of cortical perineuronal nets in focal cerebral ischemia and mild hypoperfusion. *Matrix Biol.* 2018;74:121–32. <https://doi.org/10.1016/j.matbio.2018.08.001>.
- Faini G, Aguirre A, Landi S, Lamers D, Pizzorusso T, Ratto GM, et al. Perineuronal nets control visual input via thalamic recruitment of cortical PV interneurons. *Elife.* 2018;7. <https://doi.org/10.7554/eLife.41520>.
- Favuzzi E, Marques-Smith A, Fernandes C, Ewers H, Correspondence BR. Activity-dependent gating of parvalbumin interneuron function by the perineuronal net protein brevican. *Neuron.* 2017;95:639–55. <https://doi.org/10.1016/j.neuron.2017.06.028>.
- Fawcett JW, Oohashi T, Pizzorusso T. The roles of perineuronal nets and the perinodal extracellular matrix in neuronal function. *Nat Rev Neurosci.* 2019;20:451–65. <https://doi.org/10.1038/s41583-019-0196-3>.
- Franchi SA, Macco R, Astro V, Tonoli D, Savino E, Valtorta F, et al. A method to culture GABAergic interneurons derived from the medial ganglionic eminence. *Front Cell Neurosci.* 2018;11:1–21. <https://doi.org/10.3389/fncel.2017.00423>.
- Fredriksson L, Stevenson TK, Su EJ, Ragsdale M, Moore S, Craciun S, et al. Identification of a neurovascular signaling pathway regulating seizures in mice. *Ann Clin Transl Neurol.* 2015;2:722–38. <https://doi.org/10.1002/acn3.209>.
- Frischknecht R, Heine M, Perrais D, Seidenbecher CI, Choquet D, Gundelfinger ED. Brain extracellular matrix affects AMPA receptor lateral mobility and short-term synaptic plasticity. *Nat Neurosci.* 2009;12:897–904. <https://doi.org/10.1038/nn.2338>.
- Gogolla N, Caroni P, Lüthi A, Herry C. Perineuronal nets protect fear memories from erasure. *Science.* 2009;325:1258–61. <https://doi.org/10.1126/science.1174146>.
- Hayani H, Song I, Dityatev A. Increased excitability and reduced excitatory synaptic input into fast-spiking CA2 interneurons after enzymatic attenuation of extracellular matrix. *Front Cell Neurosci.* 2018;12. <https://doi.org/10.3389/fncel.2018.00149>.
- Hébert M, Anfray A, Chevillet A, Martinez de Lizarrondo S, Quenault A, Louessard M, et al. Distant space processing is controlled by tPA-dependent NMDA receptor signaling in the entorhinal cortex. *Cereb Cortex.* 2017;27:4783–96. <https://doi.org/10.1093/cercor/bhw275>.
- Hippenmeyer S, Vrieseling E, Sigrist M, Portmann T, Laengle C, Ladle DR, et al. A developmental switch in the response of DRG neurons to ETS transcription factor signaling. *PLoS Biol.* 2005;3:0878–90. <https://doi.org/10.1371/journal.pbio.0030159>.
- Howell MD, Gottschall PE. Lectican proteoglycans, their cleaving metalloproteinases, and plasticity in the central nervous system extracellular microenvironment. *Neuroscience.* 2012;217:6–18. <https://doi.org/10.1016/j.neuroscience.2012.05.034>.
- Hu H, Gan J, Jonas P. Fast-spiking, parvalbumin+ GABAergic interneurons: from cellular design to microcircuit function. *Science.* 2014;345:1255263. <https://doi.org/10.1126/science.1255263>.
- Kawaguchi Y. Physiological, morphological, and histochemical characterization of three classes of interneurons in rat neostriatum. *J Neurosci.* 1993;13:4908–23. <https://doi.org/10.1523/jneurosci.13-11-04908.1993>.



37. Kelly EA, Russo AS, Jackson CD, Lamantia CEL, Majewska AK. Proteolytic regulation of synaptic plasticity in the mouse primary visual cortex: analysis of matrix metalloproteinase 9 deficient mice. *Front Cell Neurosci.* 2015;9:1–17. <https://doi.org/10.3389/fncel.2015.00369>.
38. Kenagy RD, Fischer JW, Davies MG, Berceli SA, Hawkins SM, Wight TN, et al. Increased plasmin and serine proteinase activity during flow-induced intimal atrophy in baboon PTFE grafts. *Arterioscler Thromb Vasc Biol.* 2002;22:400–4. <https://doi.org/10.1161/hq0302.105376>.
39. Lambolez B, Audinat E, Bochet P, Crépel F, Rossier J. AMPA receptor subunits expressed by single purkinje cells. *Neuron.* 1992;9:247–58. [https://doi.org/10.1016/0896-6273\(92\)90164-9](https://doi.org/10.1016/0896-6273(92)90164-9).
40. Lemarchant S, Pomeschik Y, Kidin I, Kärkkäinen V, Valonen P, Lehtonen S, et al. ADAMTS-4 promotes neurodegeneration in a mouse model of amyotrophic lateral sclerosis. *Mol Neurodegener.* 2016;11:1–24. <https://doi.org/10.1186/s13024-016-0078-3>.
41. Lemarchant S, Pruvost M, Hébert M, Gauberti M, Hommet Y, Briens A, et al. TPA promotes ADAMTS-4-induced CSPG degradation, thereby enhancing neuroplasticity following spinal cord injury. *Neurobiol Dis.* 2014;66:28–42. <https://doi.org/10.1016/j.nbd.2014.02.005>.
42. Lensjø KK, Lepperød ME, Dick G, Hafting T, Fyhn M. Removal of perineuronal nets unlocks juvenile plasticity through network mechanisms of decreased inhibition and increased gamma activity. *J Neurosci.* 2017;37:1269–83. <https://doi.org/10.1523/JNEUROSCI.2504-16.2016>.
43. Leonetti C, Macrez R, Pruvost M, Hommet Y, Bronsard J, Fournier A, et al. Tissue-type plasminogen activator exerts EGF-like chemokinetic effects on oligodendrocytes in white matter (re)myelination. *Mol Neurodegener.* 2017;12:1–16. <https://doi.org/10.1186/s13024-017-0160-5>.
44. Liot G, Roussel BD, Lebeurrier N, Benchenane K, López-Atalaya JP, Vivien D, et al. Tissue-type plasminogen activator rescues neurones from serum deprivation-induced apoptosis through a mechanism independent of its proteolytic activity. *J Neurochem.* 2006;98:1458–64. <https://doi.org/10.1111/j.1471-4159.2006.03982.x>.
45. Louessard M, Bardou I, Lemarchand E, Thiebaut AM, Parcq J, Leprince J, et al. Activation of cell surface GRP78 decreases endoplasmic reticulum stress and neuronal death. *Cell Death Differ.* 2017;24:1518–29. <https://doi.org/10.1038/cdd.2017.35>.
46. Louessard M, Lacroix A, Martineau M, Mondielli G, Montagne A, Lesept F, et al. Tissue plasminogen activator expression is restricted to subsets of excitatory pyramidal glutamatergic neurons. *Mol Neurobiol.* 2016;53:5000–12. <https://doi.org/10.1007/s12035-015-9432-7>.
47. Macrez R, Ortega MC, Bardou I, Mehra A, Fournier A, Van der Pol SMA, et al. Neuroendothelial NMDA receptors as therapeutic targets in experimental autoimmune encephalomyelitis. *Brain.* 2016;139:2406–19. <https://doi.org/10.1093/brain/aww172>.
48. Madani R, Hulo S, Toni N, Madani H, Steimer T, Muller D, et al. Enhanced hippocampal long-term potentiation and learning by increased neuronal expression of tissue-type plasminogen activator in transgenic mice. *EMBO J.* 1999;18:3007–12. <https://doi.org/10.1093/emboj/18.11.3007>.
49. Madinier A, Quattromani MJ, Sjölund C, Ruscher K, Wieloch T. Enriched housing enhances recovery of limb placement ability and reduces aggrecan-containing perineuronal nets in the rat somatosensory cortex after experimental stroke. *PLoS One.* 2014;9:1–14. <https://doi.org/10.1371/journal.pone.0093121>.
50. Maes ME, Colombo G, Schulz R, Siegert S. Targeting microglia with lentivirus and AAV: recent advances and remaining challenges. *Neurosci Lett.* 2019;707:1–10. <https://doi.org/10.1016/j.neulet.2019.134310>.
51. Mascio G, Bucci D, Notartomaso S, Liberatore F, Antenucci N, Scarselli P, et al. Perineuronal nets are under the control of type-5 metabotropic glutamate receptors in the developing somatosensory cortex. *Transl Psychiatry.* 2021;11. <https://doi.org/10.1038/s41398-021-01210-3>.
52. Mataga N, Mizuguchi Y, Hensch TK. Experience-dependent pruning of dendritic spines in visual cortex by tissue plasminogen activator. *Neuron.* 2004;44:1031–41. <https://doi.org/10.1016/j.neuron.2004.11.028>.
53. Mataga N, Nagai N, Hensch TK. Permissive proteolytic activity for visual cortical plasticity. *Proc Natl Acad Sci U S A.* 2002;99:7717–21. <https://doi.org/10.1073/pnas.102088899>.
54. Matys T, Pawlak R, Matys E, Pavlides C, McEwen BS, Strickland S. Tissue plasminogen activator promotes the effects of corticotropin-releasing factor on the amygdala and anxiety-like behavior. *Proc Natl Acad Sci U S A.* 2004;101:16345–50. <https://doi.org/10.1073/pnas.0407355101>.
55. Mehra A, Guérit S, Macrez R, Gosselet F, Sevin E, Lebas H, et al. Nonionotropic action of endothelial NMDA receptors on blood–brain barrier permeability via Rho/ROCK-mediated phosphorylation of myosin. *J Neurosci.* 2020;40:1778–87. <https://doi.org/10.1523/JNEUROSCI.0969-19.2019>.
56. Merienne N, Le Douce J, Faivre E, Déglon N, Bonvento G. Efficient gene delivery and selective transduction of astrocytes in the mammalian brain using viral vectors. *Front Cell Neurosci.* 2013;7:1–13. <https://doi.org/10.3389/fncel.2013.00106>.
57. Miyata S, Nishimura Y, Nakashima T. Perineuronal nets protect against amyloid  $\beta$ -protein neurotoxicity in cultured cortical neurons. *Brain Res.* 2007;1150:200–6. <https://doi.org/10.1016/j.brainres.2007.02.066>.
58. Müller CM, Griesinger CB. Tissue plasminogen activator mediates reverse occlusion plasticity in visual cortex. *Nat Neurosci.* 1998;1:47–53. <https://doi.org/10.1038/248>.
59. Murase S, Lantz CL, Quinlan EM. Light reintroduction after dark exposure reactivates plasticity in adults via perisynaptic activation of MMP-9. *Elife.* 2017;6:1–23. <https://doi.org/10.7554/eLife.27345>.
60. Nakamura M, Nakano K, Morita S, Nakashima T, Oohira A, Miyata S. Expression of chondroitin sulfate proteoglycans in barrel field of mouse and rat somatosensory cortex. *Brain Res.* 2009;1252:117–29. <https://doi.org/10.1016/j.brainres.2008.11.022>.
61. Nicole O, Docagne F, Ali C, Margail I, Carmeliet P, MacKenzie ET, et al. The proteolytic activity of tissue-plasminogen activator enhances NMDA receptor-mediated signaling. *Nat Med.* 2001;7:59–64. <https://doi.org/10.1038/83358>.
62. Orlando C, Ster J, Gerber U, Fawcett JW, Raineteau O. Perisynaptic chondroitin sulfate proteoglycans restrict structural plasticity in an integrin-dependent manner. *J Neurosci.* 2012;32:18009–17. <https://doi.org/10.1523/JNEUROSCI.2406-12.2012>.
63. Pantazopoulos H, Gisabella B, Rexrode L, Benefield D, Yildiz E, Seltzer P, et al. Circadian rhythms of perineuronal net composition. *eNeuro.* 2020;7:1–21. <https://doi.org/10.1523/ENEURO.0034-19.2020>.
64. Pasquet N, Douceau S, Naveau M, Lesept F, Louessard M, Leboviev L, et al. Tissue-type plasminogen activator controlled corticogenesis through a mechanism dependent of NMDA receptors expressed on radial glial cells. *Cereb Cortex.* 2019;29:2482–98. <https://doi.org/10.1093/cercor/bhy119>.
65. Pawlak R, Magarinos AM, Melchor J, McEwen B, Strickland S. Tissue plasminogen activator in the amygdala is critical for stress-induced anxiety-like behavior. *Nat Neurosci.* 2003;6:168–74. <https://doi.org/10.1038/nn998>.
66. Pizzorusso T, Medini P, Berardi N, Chierzi S, Fawcett JW, Maffei L. Reactivation of ocular dominance plasticity in the adult visual cortex. *Science.* 2002;298:1248–51. <https://doi.org/10.1126/science.1072699>.
67. Pu H, Shi Y, Zhang L, Lu Z, Ye Q, Leak RK, et al. Protease-independent action of tissue plasminogen activator in brain plasticity and neurological recovery after ischemic stroke. *Proc Natl Acad Sci U S A.* 2019;116:9115–24. <https://doi.org/10.1073/pnas.1821979116>.
68. Qian Z, Gilbert ME, Colicos MA, Kandel ER, Kuhl D. Tissue-plasminogen activator is induced as an immediate-early gene during seizure, kindling and long-term potentiation. *Nature.* 1993;361:453–7. <https://doi.org/10.1038/361453a0>.
69. Reinhard SM, Rais M, Afroz S, Hanania Y, Pendi K, Espinoza K, et al. Reduced perineuronal net expression in Fmr1 KO mice auditory cortex and amygdala is linked to impaired fear-associated memory. *Neurobiol Learn Mem.* 2019;164. <https://doi.org/10.1016/j.nlm.2019.107042>.
70. Romberg C, Yang S, Melani R, Andrews MR, Horner AE, Spillantini MG, et al. Depletion of perineuronal nets enhances recognition memory and long-term depression in the perirhinal cortex. *J Neurosci.* 2013;33:7057–65. <https://doi.org/10.1523/JNEUROSCI.6267-11.2013>.
71. Rossier J, Bernard A, Cabungcal JH, Perrenoud Q, Savoye A, Gallopin T, et al. Cortical fast-spiking parvalbumin interneurons enwrapped in the perineuronal net express the metalloproteinases Adamts8, Adamts15 and Nephrilysin. *Mol Psychiatry.* 2015;20:154–61. <https://doi.org/10.1038/mp.2014.162>.
72. Rowlands D, Lensjø KK, Dinh T, Yang S, Andrews MR, Hafting T, et al. Aggrecan directs extracellular matrix-mediated neuronal plasticity. *J Neurosci.* 2018;38:10102–13. <https://doi.org/10.1523/JNEUROSCI.1122-18.2018>.

73. Ruden JB, Dugan LL, Konradi C. Parvalbumin interneuron vulnerability and brain disorders. *Neuropsychopharmacology*. 2021;46:279–87. <https://doi.org/10.1038/s41386-020-0778-9>.
74. Sallés FJ, Strickland S, Sallés FJ, Strickland S. Localization and regulation of the tissue plasminogen activator-plasmin system in the hippocampus. *J Neurosci*. 2002;22:2125–34. <https://doi.org/10.1523/jneurosci.22-06-02125.2002>.
75. Sappino AP, Madani R, Huarte J, Belin D, Kiss JZ, Wohlwend A, et al. Extracellular proteolysis in the adult murine brain. *J Clin Invest*. 1993;92:679–85. <https://doi.org/10.1172/JCI116637>.
76. Shi W, Wei X, Wang X, Du S, Liu W, Song J, et al. Perineuronal nets protect long-term memory by limiting activity-dependent inhibition from parvalbumin interneurons. *Proc Natl Acad Sci U S A*. 2019;116:27063–73. <https://doi.org/10.1073/pnas.1902680116>.
77. Siao CJ, Tsirka SE. Tissue plasminogen activator mediates microglial activation via its finger domain through annexin II. *J Neurosci*. 2002;22:3352–8. <https://doi.org/10.1523/jneurosci.22-09-03352.2002>.
78. Slaker M, Churchill L, Todd RP, Blacktop JM, Zuloaga DG, Raber J, et al. Removal of perineuronal nets in the medial prefrontal cortex impairs the acquisition and reconsolidation of a cocaine-induced conditioned place preference memory. *J Neurosci*. 2015;35:4190–202. <https://doi.org/10.1523/JNEUROSCI.3592-14.2015>.
79. Sparta DR, Hovelsø N, Mason AO, Kantak PA, Ung RL, Decot HK, et al. Activation of prefrontal cortical parvalbumin interneurons facilitates extinction of reward-seeking behavior. *J Neurosci*. 2014;34:3699–705. <https://doi.org/10.1523/JNEUROSCI.0235-13.2014>.
80. Stevenson TK, Lawrence DA. Characterization of tissue plasminogen activator expression and trafficking in the adult murine brain. *eNeuro*. 2018;5:1–18. <https://doi.org/10.1523/ENEURO.0119-18.2018>.
81. Su EJ, Fredriksson L, Geyer M, Folestad E, Cale J, Andrae J, et al. Activation of PDGF-CC by tissue plasminogen activator impairs blood-brain barrier integrity during ischemic stroke. *Nat Med*. 2008;14:731–7. <https://doi.org/10.1038/nm1787>.
82. Sumi Y, Dent MA, Owen DE, Seeley PJ, Morris RJ. The expression of tissue and urokinase-type plasminogen activators in neural development suggests different modes of proteolytic involvement in neuronal growth. *Development*. 1992;116:625–37.
83. Sur M, Frost DO, Hockfield S. Expression of a surface-associated antigen on Y-cells in the cat lateral geniculate nucleus is regulated by visual experience. *J Neurosci*. 1988;8:874–82. <https://doi.org/10.1523/jneurosci.08-03-00874.1988>.
84. Teesalu T, Kulla A, Asser T, Koskiniemi M, Vaheri A. Tissue plasminogen activator as a key effector in neurobiology and neuropathology. *Biochem Soc Trans*. 2002;30:183–9. <https://doi.org/10.1042/bst0300183>.
85. Teesalu T, Kulla A, Simisker A, Sirén V, Lawrence DA, Asser T, et al. Tissue plasminogen activator and neuroserpin are widely expressed in the human central nervous system. *Thromb Haemost*. 2004. <https://doi.org/10.1160/th02-12-0310>.
86. Testa D, Prochiantz A, Di Nardo AA. Perineuronal nets in brain physiology and disease. *Semin Cell Dev Biol*. 2019;89:125–35. <https://doi.org/10.1016/j.semcdb.2018.09.011>.
87. Thiebaut AM, Gauberti M, Ali C, Martinez De Lizarrondo S, Vivien D, Yepes M, et al. The role of plasminogen activators in stroke treatment: fibrinolysis and beyond. *Lancet Neurol*. 2018;17:1121–32. [https://doi.org/10.1016/S1474-4422\(18\)30323-5](https://doi.org/10.1016/S1474-4422(18)30323-5).
88. Thorndike RL. Who belongs in the family? *Psychometrika*. 1953;18:267–76. <https://doi.org/10.1007/BF02289263>.
89. Ueno H, Suemitsu S, Okamoto M, Matsumoto Y, Ishihara T. Sensory experience-dependent formation of perineuronal nets and expression of Cat-315 immunoreactive components in the mouse somatosensory cortex. *Neuroscience*. 2017;355:161–74. <https://doi.org/10.1016/j.neuroscience.2017.04.041>.
90. Visse R, Nagase H. Matrix metalloproteinases and tissue inhibitors of metalloproteinases: structure, function, and biochemistry. *Circ Res*. 2003;92:827–39. <https://doi.org/10.1161/01.RES.0000070112.80711.3D>.
91. Wang W-Y, Xu G-Z, Tian J, Sprecher AJ. Inhibitory effect on LPS-induced retinal microglial activation of downregulation of t-PA expression by siRNA interference. *Curr Eye Res*. 2009;34:476–84. <https://doi.org/10.1080/02713680902916108>.
92. Ward JH. Hierarchical grouping to optimize an objective function. *J Am Stat Assoc*. 1963;58:236–44. <https://doi.org/10.1080/01621459.1963.10500845>.
93. Wen TH, Binder DK, Ethell IM, Razak KA. The perineuronal 'safety' net? Perineuronal net abnormalities in neurological disorders. *Front Mol Neurosci*. 2018;11:270.
94. Wu F, Wu J, Nicholson AD, Echeverry R, Haile WB, Catano M, et al. Tissue-type plasminogen activator regulates the neuronal uptake of glucose in the ischemic brain. *J Neurosci*. 2012;32:9848–58. <https://doi.org/10.1523/JNEUROSCI.1241-12.2012>.
95. Wu YP, Siao CJ, Lu W, Sung TC, Frohman MA, Milev P, et al. The tissue plasminogen activator regulates the neuronal proteolytic system regulates seizure-induced hippocampal mossy fiber outgrowth through a proteoglycan substrate. *J Cell Biol*. 2000;148:1295–304. <https://doi.org/10.1083/jcb.148.6.1295>.
96. Ye Q, Miao Q, Long (2013) Experience-dependent development of perineuronal nets and chondroitin sulfate proteoglycan receptors in mouse visual cortex. *Matrix Biol* 32:352–363. <https://doi.org/10.1016/j.matbio.2013.04.001>
97. Yutsudo N, Kitagawa H. Involvement of chondroitin 6-sulfation in temporal lobe epilepsy. *Exp Neurol*. 2015;274:126–33. <https://doi.org/10.1016/j.expneurol.2015.07.009>.
98. Zhu J, Wan Y, Xu H, Wu Y, Hu B, Jin H. The role of endogenous tissue-type plasminogen activator in neuronal survival after ischemic stroke: friend or foe? *Cell Mol Life Sci*. 2019;76:1489–506. <https://doi.org/10.1007/s00018-019-03005-8>.

## Publisher's Note

Springer Nature remains neutral with regard to jurisdictional claims in published maps and institutional affiliations.

Ready to submit your research? Choose BMC and benefit from:

- fast, convenient online submission
- thorough peer review by experienced researchers in your field
- rapid publication on acceptance
- support for research data, including large and complex data types
- gold Open Access which fosters wider collaboration and increased citations
- maximum visibility for your research: over 100M website views per year

At BMC, research is always in progress.

Learn more [biomedcentral.com/submissions](https://biomedcentral.com/submissions)

